



## Slamming Probability and Impact to Speedboats Hull Based on Seakeeping Motion

Amalia Ika Wulandari<sup>1\*)</sup>, Husein Syahab<sup>1)</sup>, Berlian Arswendo Adietya<sup>2)</sup>

<sup>1)</sup>Departement of Naval Architecture, Institut Teknologi Kalimantan, Balikpapan, Indonesia

<sup>2)</sup>Departement of Naval Architecture, Universitas Diponegoro, Semarang, Indonesia

<sup>\*)</sup>Corresponding Author: [amalaiakaw@lecturer.itk.ac.id](mailto:amalaiakaw@lecturer.itk.ac.id)

### Article Info

### Abstract

#### Keywords:

Boundary Element Method (BEM);  
Finite Element Method (FEM);  
Probabilistic;  
Slamming;  
Small Craft.

#### Article history:

Received: 21/09/2025  
Last revised: 01/11/2025  
Accepted: 08/11/2025  
Available online: 09/11/2025  
Published: 09/11/2025

#### DOI:

<https://doi.org/10.14710/kapal.v22i3.77940>

Slamming is a critical dynamic load for small, high-speed craft because repeated hull-wave impacts can generate intense stresses and deformations that threaten structural integrity. This study investigates the probabilistic risk of slamming and the resulting structural response of an aluminium speedboat by integrating seakeeping motion analysis with structural evaluation. First, vessel motions and wave-induced pressures were computed using the Boundary Element Method (BEM) under regular wave conditions with significant heights of 0.125 m, 0.25 m, and 0.50 m. Heave and pitch motions were quantified through Response Amplitude Operators, and their statistics were used to estimate the probability of bottom slamming. The probability associated with pitch increased from 54 % at 0.125 m to 86 % at 0.50 m, showing that pitch is the dominant trigger for slamming. The calculated hydrodynamic pressures were then applied to a detailed Finite Element Method (FEM) model of the aluminium hull to evaluate structural stresses and deformations. As wave height increased from 0.125 m to 0.50 m, the maximum slamming load rose from  $2.28 \times 10^{-3}$  MPa to  $9.10 \times 10^{-3}$  MPa, causing peak structural stresses to climb from 4.77 MPa to 19.06 MPa and maximum deformations from 0.19 mm to 0.76 mm. Stress concentrations were consistently located on unsupported bottom plating near the bow, while areas reinforced by transverse frames experienced much lower response. These findings demonstrate that both sea-state severity and hull reinforcement layout govern slamming vulnerability, providing practical guidance for strengthening small craft against impulsive wave impacts.

Copyright © 2025 KAPAL: Jurnal Ilmu Pengetahuan dan Teknologi Kelautan. This is an open access article under the CC BY-SA license (<https://creativecommons.org/licenses/by-sa/4.0/>).

## 1. Introduction

Slamming is a violent hydrodynamic phenomenon that occurs when a vessel's hull re-enters the water with significant relative velocity, producing short-duration, high-magnitude pressures. These impulsive loads can excite global hull vibrations, induce local structural stresses, and accelerate fatigue damage, making slamming a critical consideration for naval architects and marine engineers. Although all seagoing vessels are exposed to slamming to some degree, the risk is particularly acute for small, high-speed craft such as patrol boats and recreational speedboats. Their lightweight construction, shallow draft, and limited structural redundancy amplify the impact of repeated wave-hull interactions, especially in moderate to rough seas where planning or semi-planning conditions prevail.

Fast patrol and leisure craft often operate at high Froude numbers, where the likelihood of bow or bottom impacts with steep waves is elevated. Rahmaji et al. [1] emphasize that improving resistance, stability, and seakeeping is central to the design of fast patrol boats, yet even optimized hull forms remain vulnerable to slamming loads when driven at speed in adverse conditions. Pegorari [2] and Thodal [3] both underscore that composite and aluminium construction, while advantageous for weight reduction, can exacerbate the structural consequences of slamming because of lower inherent damping and stiffness compared to steel. Understanding the combined hydrodynamic and structural mechanisms of slamming is therefore essential for the safe and durable design of small craft.

Although slamming has been widely investigated, most research still isolates the hydrodynamic excitation from the resulting structural response instead of treating them as a single motion-impact process. Truong et al. [4], for example, benchmarked the transient response of flat-stiffened plates subjected to fluid-structure interaction and clarified how short-duration loads excite complex structural vibrations. Expanding on localized impact effects, Gao and Zhou [5] used three-dimensional fluid-structure interaction simulations to examine bow-slamming pressures, demonstrating that parameters such as vessel speed, entry angle, and draft depth strongly govern impact intensity. Material-focused strategies have also been explored. Mousavi and Khoob [6] numerically evaluated steel-concrete-steel composite plates reinforced with ultra-lightweight, high-ductility cementitious layers, showing notable reductions in strain and stress transfer during bottom-slamming events, yet their work did not address the vessel motions or sea states that precipitate such impacts. Experimental

contributions include Li et al. [7], who tested a segmented cruise-ship model to study stern slamming, revealing that small longitudinal deadrise angles in following seas can produce large impact loads and induce hull-girder whipping. Nevertheless, that study remained confined to physical testing and lacked numerical modelling for broader applicability.

Taken together, these investigations enrich understanding of local slamming loads and structural reactions, but they also underscore a key research gap: the integration of seakeeping motion analysis with probabilistic impact risk and structural assessment—an especially critical need for lightweight small craft prone to repeated slamming in moderate to rough seas.

While fully coupled two-way fluid–structure interaction offers the highest fidelity, it is computationally intensive for routine design. A one-way fluid–structure strategy provides a practical alternative, in which hydrodynamic pressures derived from seakeeping analysis serve as external loads in a detailed structural model [8]. For the hydrodynamic component, the Boundary Element Method (BEM) is widely used to predict ship motions and wave-induced pressures, efficiently capturing heave and pitch responses under various sea states [9]. These pressures can then be transferred to a Finite Element Method (FEM) model to compute stress distributions and deformations with high spatial resolution [10,11]. This sequential BEM–FEM framework allows rigorous assessment of slamming-induced structural effects while maintaining computational efficiency.

This study applies such an integrated numerical approach to evaluate the slamming probability and structural response of an aluminium speedboat. First, vessel motions and wave-induced pressures are computed using BEM under regular waves of varying significant heights to quantify heave and pitch statistics and estimate bottom-slamming probability. The calculated hydrodynamic pressures are subsequently applied to a detailed FEM model to assess stress distributions and deformations. By linking seakeeping motion analysis with structural evaluation in a one-way fluid–structure framework, this work provides a comprehensive understanding of how sea-state severity and hull-reinforcement layout govern slamming vulnerability, offering practical guidance for the design and strengthening of small, high-speed craft.

## 2. Method

### 2.1. Research Framework

This study adopts a sequential, one-way fluid–structure methodology that links seakeeping motion analysis with detailed structural evaluation. The process begins with the creation of a three-dimensional digital model of the aluminium speedboat, including its hull geometry, material properties, and internal stiffening arrangement. This model serves as the foundation for both the hydrodynamic and structural simulations. The hydrodynamic stage uses the Boundary Element Method (BEM) to compute wave-induced pressures and motion responses under regular waves with significant heights of 0.125 m, 0.25 m, and 0.50 m, representing mild to moderate sea states. From these simulations, the vessel's heave and pitch motions are expressed through Response Amplitude Operators. Statistical analysis of the resulting time series provides estimates of bottom-slamming probability, clarifying how vessel speed, wave frequency, and heading combine to influence the likelihood of hull–wave impacts.

Hydrodynamic pressure distributions corresponding to peak slamming conditions are then extracted from the BEM output and applied as boundary loads in a high-fidelity Finite Element Method (FEM) model of the hull. This structural model captures the arrangement of transverse frames, stiffeners, and plating so that stresses and deformations can be evaluated with precision. By subjecting the FEM model to the simulated slamming pressures, the analysis identifies stress concentrations and maximum displacements, highlighting vulnerable areas such as unsupported bottom plating near the bow and providing guidance for potential reinforcement strategies. This integrated approach offers several key strengths. Coupling BEM-based motion prediction with FEM structural analysis links seakeeping behaviour directly to structural response while maintaining computational efficiency. Incorporating probabilistic slamming assessment from motion statistics enables risk-based evaluation rather than relying solely on deterministic worst-case scenarios. The one-way coupling also reduces computational cost compared with fully coupled fluid–structure interaction yet provides sufficient accuracy for engineering decisions and practical design recommendations.

Nevertheless, certain limitations must be acknowledged. Because the approach assumes one-way coupling, structural deformations are not fed back into the hydrodynamic calculations, so any influence of hull flexibility on the pressure field is neglected. The use of regular-wave conditions simplifies the stochastic nature of real seas and does not fully represent multi-directional or irregular wave spectra. In addition, the FEM analysis assumes linear-elastic material behavior and simplified damping properties, which may underestimate nonlinear or fatigue effects in aluminum structures. Finally, while the numerical simulations are validated against established theory, scaling to full-scale operational conditions requires additional verification to account for Reynolds number effects and complex sea spectra. The absence of experimental validation, such as model tests or full-scale measurements, introduces uncertainty in predictive accuracy a challenge highlighted in related slamming studies [7]. Furthermore, the reliance on linear assumptions and regular wave conditions restricts applicability to more complex sea states, where nonlinearities and irregular, multidirectional spectra can significantly alter slamming frequency and intensity [12]. In addition, as noted in prior works [13 – 20], help mitigate the limitation of material experimental validation, offering reference measurements and comparative benchmarks that strengthen confidence in the FEM results.

### 2.2. Study Objects and Operational Condition

Accurate three-dimensional (3D) hull modelling is the foundation of both the hydrodynamic and structural analyses in this study. The process begins with defining the principal dimensions of the speedboat, shown in Table 1, based on design drawings or hydrostatic plans. The hull geometry is generated by lofting a series of transverse and longitudinal curves to

produce a fair surface free of abrupt curvature changes. Special attention is paid to critical features such as the bow flare, chine lines, and transom, as these influence both seakeeping performance and slamming susceptibility. After the outer shell is defined, internal structural elements including transverse frames, longitudinal girders, and deck supports are incorporated to ensure that the model represents the actual load-bearing configuration. This model shown in [Figure 1](#).

To support hydrodynamic analysis, the final surface model is exported in a mesh or panelised format compatible with the Boundary Element Method (BEM), ensuring that the discretization captures fine details near the bow and bottom plating where pressure gradients are steep. For structural evaluation, the same geometry is imported into finite element software and converted into a solid or shell-element mesh, with mesh refinement applied in regions expected to experience high slamming loads. This dual-purpose 3D model allows seamless transfer of hydrodynamic pressure fields to the finite element model, enabling consistent evaluation of motions, slamming pressures, and structural responses. By carefully building and validating the 3D geometry, the modelling process ensures that both the seakeeping simulations and the structural analyses are based on an accurate and realistic representation of the small craft hull [21]. Aluminium alloys are highly regarded due to their favourable strength-to-weight ratio, natural corrosion resistance, and ease of fabrication characteristics that make them a primary option for small craft design [13]. Aluminium has become a preferred material in small craft construction owing to its high mechanical efficiency, seawater corrosion resistance, and ease of fabrication [20]. Widely used marine-grade alloys such as 5083 and 6061 combine strong mechanical properties with excellent weldability, enabling weight reduction while maintaining structural integrity. The chosen material properties are summarized in [Table 2](#). These parameters represent the fundamental inputs for evaluating the structural performance of the vessel when subjected to wave-induced loads.

Table 1. Main Particulars of the Small Craft

Dimension	Size	Unit
Length	6.041	m
Width	2.432	m
Height	1.795	m

Table 2. Material Characteristics of Aluminum

Properties	Magnitude	Unit
Density	2700	Kg/m <sup>3</sup>
Young's Modulus	68900	MPa
Ultimate Tensile Strength	165	MPa
Poisson's Ratio	0.33	-

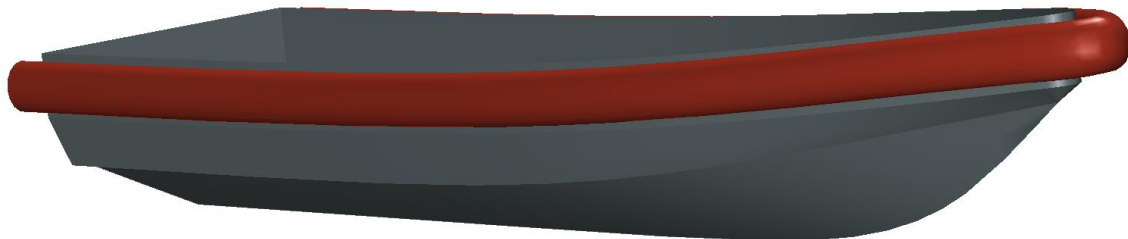


Figure 1. 3D modeling of ship model

The study models the vessel's service environment by simulating several representative sea states. [Figure 2](#) shows the significant wave heights used as key parameters for evaluating how different sea levels might affect the hull's structural behaviour within its expected operating region [22]. To capture directional influences, the analysis also incorporates three incident-wave heading namely 0° (following seas), 90° (beam seas), and 180° (head seas) as depicted in [Figure 3](#).

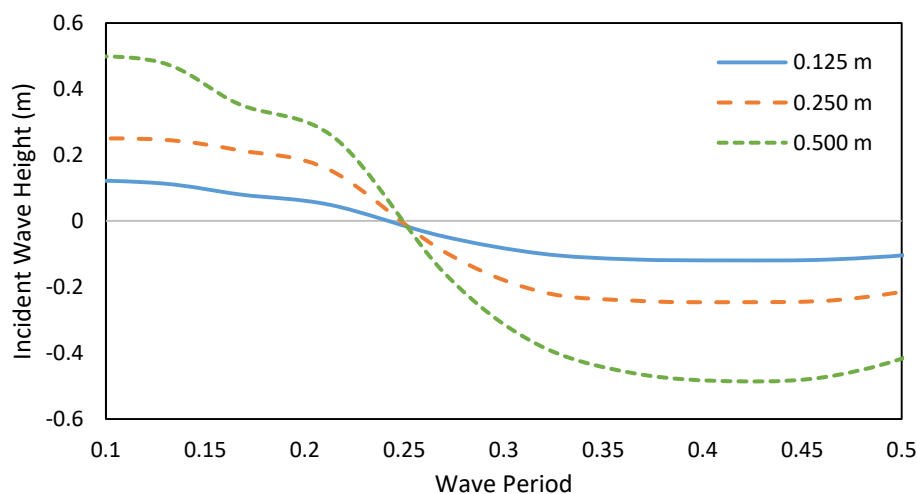


Figure 2. Comparison Across Incident Wave Heights

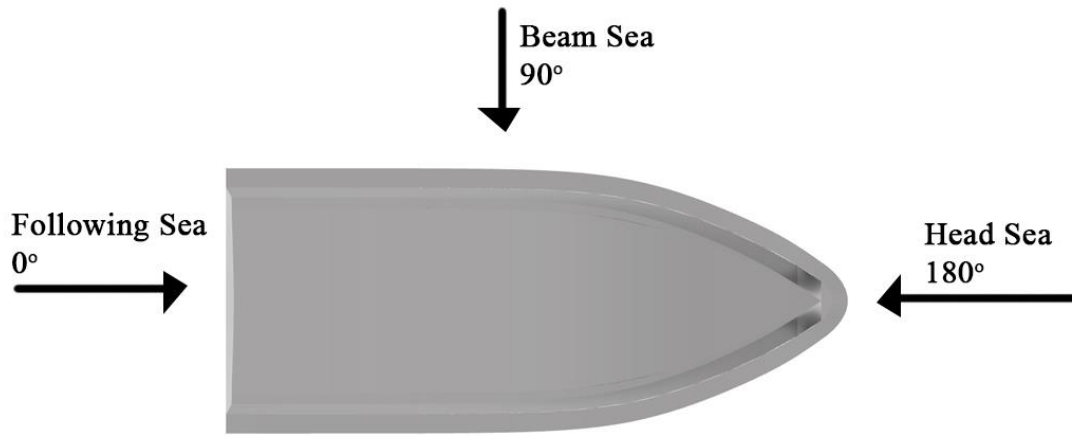


Figure 3. Heading of wave encountered by ship

### 2.3. Hydrodynamic Analysis

This study employs two complementary numerical methods to assess the hydrodynamic behaviour and structure strength of boat hull against wave load: BEM for hydrodynamic analysis and the FEM for structural evaluation. BEM provides an efficient means of estimating vessel motions and wave-induced hydrodynamic forces. Unlike FEM, which discretizes the full structural domain and directly solves the governing partial differential equations, BEM reformulates the problem into boundary integrals. This reduces computational dimensionality, as only the wetted hull surface requires discretization. Such simplification is particularly beneficial for wave-structure interaction problems, as it streamlines the meshing process and is well-suited for modelling unbounded fluid domains such as the open sea [23].

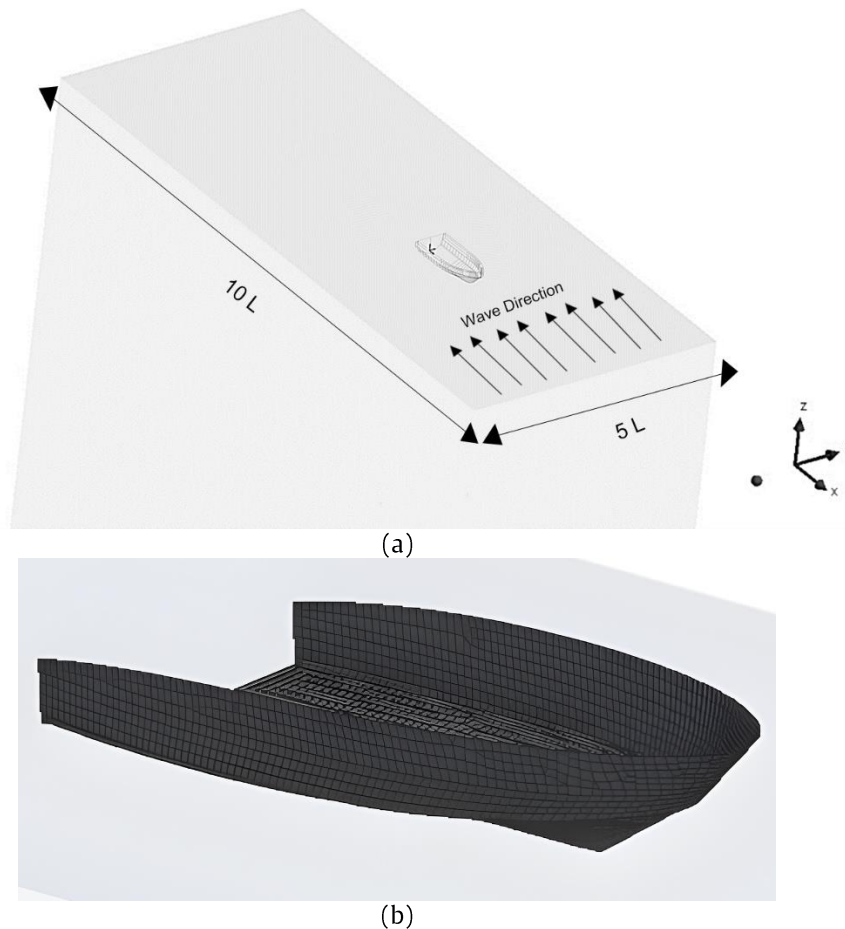


Figure 4. Configuration of hydrodynamic analysis with Boundary Element Method (BEM): (a) boundary conditions, (b) hull mesh

The dynamic response of the vessel is governed by the interaction between incoming wave fields and the submerged hull geometry. As the craft oscillates, variations in the wetted surface modify the pressure distribution along the hull, which in turn influences both motion responses and internal structural loading. In the hydrodynamic model, the flow is assumed to be inviscid, incompressible, and irrotational, leading to the Laplace equation for the velocity potential,  $\phi$ , as expressed in Eq. (1).

$$\nabla^2 \phi = 0 \quad (1)$$

In Cartesian coordinates ( $x,y,z$ ), the Laplace equation expands to Eq. (2). The Appropriate boundary conditions are enforced on the free surface, hull boundary, and seabed. For example, at the seabed, a no-flux condition is applied as in Eq. (3).

$$\frac{\partial^2 \phi}{\partial x^2} + \frac{\partial^2 \phi}{\partial y^2} + \frac{\partial^2 \phi}{\partial z^2} \quad (2)$$

$$\frac{\partial \phi}{\partial z} = 0 \quad (3)$$

The computational domain employed in this study is shown in Figure 4. It was configured with an overall length of  $10L$  and a width of  $5L$ , where  $L$  represents the vessel's length. The upstream boundary was positioned  $2L$  ahead of the fore perpendicular (FP), while the downstream boundary extended  $7L$  beyond the aft perpendicular (AP). This setup provides adequate space for wave generation and propagation, thereby reducing the likelihood of artificial reflections and boundary effects that could otherwise compromise the accuracy of the simulation [10].

#### 2.4. Seakeeping Motion and Slamming Probability Analysis

Seakeeping analysis aims to evaluate how a ship behaves in a wave environment, particularly how it responds in terms of motion (e.g., heave, pitch, roll), acceleration, and relative displacement [24]. The key step in seakeeping calculations is to compute the Response Amplitude Operators (RAOs), which define the ratio of a specific ship motion amplitude to the wave amplitude at a given frequency as in Eq. (4).

$$RAO_j(\omega) = \frac{|\xi_j(\omega)|}{|A(\omega)|} \quad (4)$$

Where  $\xi_j(\omega)$  is the complex amplitude of motion in degree of freedom  $j$  (e.g., heave, pitch), and  $A(\omega)$  is the wave amplitude at angular frequency  $\omega$ . To evaluate how the ship performs in a realistic wave environment, irregular sea conditions are modelled using wave energy spectra such as Pierson–Moskowitz or JONSWAP [25]. In practical conditions, sea waves are irregular and can be represented as the superposition of multiple regular wave components with varying frequencies, amplitudes, and phases. When a ship moves forward at a constant speed, it encounters waves at a frequency different from their actual frequency in a stationary reference frame [26]. This results in a Doppler-like shift, where the encounter frequency  $\omega_e$  differs from the natural wave frequency  $\omega_w$ . The relationship is defined in Eq. (5).

$$\omega_e = \omega_w - \frac{g \cdot \cos \mu}{V_s} \quad (5)$$

Where  $\omega_e$  is the encounter frequency (rad/s),  $\omega_w$  is the wave frequency (rad/s),  $g$  is the gravitational acceleration ( $m/s^2$ ),  $V_s$  is the ship speed, and  $\mu$  is the wave heading ( $^\circ$ ). In the case where the vessel is at zero speed (i.e., stationary), the encounter frequency equals the wave frequency. The wave energy spectrum applied in this analysis is the Pierson–Moskowitz spectrum, commonly used to model fully developed seas. It is defined in Eq. (6).

$$S(\omega) = \frac{AH_s^2}{\omega^5} \exp\left(-\frac{B}{\omega^4 T^4}\right) \quad (6)$$

Where  $S(\omega)$  is the wave spectral density,  $H_s$  is the significant wave height,  $\omega$  is the angular wave frequency, and  $A$  and  $B$  are empirical constants. The ship's motion response in that sea condition is then statistically evaluated using spectral moments of the motion response function in Eq. (7).

$$m_n = \int_0^\infty \omega^n |A(\omega)|^2 S(\omega) d\omega \quad (7)$$

Where  $m_n$  is the  $n$ th spectral moment,  $S(\omega)$  is the wave spectral density function, and  $|RAO(\omega)|$  is the modulus of the motion RAO [27]. Structural behaviour of marine vessels under wave loading can be investigated using two principal approaches: experimental and numerical. Experimental methods, such as towing-tank testing or sea trials, provide valuable data but are often costly and time-consuming. Numerical approaches, by contrast, offer a more practical and efficient means of assessment. These methods may rely on mathematical formulations, analytical modelling, or empirical relationships; however, closed-form solutions are rarely feasible in real engineering applications due to the complexity of boundary conditions and material properties. Consequently, numerical techniques particularly the Boundary Element Method (BEM)

have emerged as an effective tool for analysing hydrodynamic behaviour with improved computational efficiency [25]. The fundamental concept of BEM is to reformulate governing equations into boundary integrals, which reduces the problem dimensionality since only the wetted hull surface needs to be discretized.

The BEM has proven especially valuable for studying the hydrodynamic responses of small craft subjected to wave-induced slamming. For lightweight vessels, such as aluminium speedboats, BEM provides a systematic framework to investigate how incident waves and hull geometry interact to generate pressure distributions, added mass, and damping effects that drive vessel motions. The modelling process typically begins with an accurate hull geometry, which is discretized along the wetted surface. Material properties and hydrodynamic boundary conditions are then applied, after which wave excitation forces and motion responses are computed. This enables evaluation of both global motions and localized hydrodynamic pressures that may contribute to structural loading [28].

One of the strengths of BEM is its ability to capture the non-uniform and time-varying pressure distributions along the wetted surface. Unlike simplified strip theory or analytical models that assume uniform loading, BEM accounts for the spatial variability of real slamming forces. This allows for more accurate analysis of critical regions such as the bow flare, bottom panels, or deck edges areas that are often most exposed to impulsive loads [29 – 31]. Furthermore, BEM supports time-domain simulations, enabling detailed examination of transient slamming events and their influence on vessel motions. This feature is particularly important for small craft, which are more susceptible to extreme accelerations and localized impacts due to their lightweight construction.

In addition to motion prediction, BEM can be applied in parametric studies to evaluate the influence of wave conditions, hull form variations, and operating speeds. Such studies provide insight not only into the likelihood of slamming events but also into how design choices affect hydrodynamic performance. By quantifying pressure distributions, wave forces, and motion responses, BEM results contribute to improved understanding of slamming phenomena and support optimization strategies for safer and more efficient small craft operation. Thus, BEM serves both as an analytical tool for investigating hydrodynamic loads and as a predictive framework for guiding design and operational decisions.

Bottom slamming occurs when the bow of the vessel rises above the water surface and subsequently re-enters, generating an impulsive hydrodynamic force within a very short time. This phenomenon is particularly critical in rough seas, as it may lead to local buckling of forward bottom plating, excessive hull girder stresses, equipment damage, and overall reduction of structural integrity. The probability can be calculated using the following expression Eq. (8), with  $T$  as vessel draft and  $M_0$  stand for RMS of each relative motions.

$$Prob_{BS} = \exp\left(-\frac{T^2}{2M_0}\right) \quad (8)$$

## 2.5. Finite Element Analysis

The Finite Element Method (FEM) is a powerful numerical approach for analyzing how marine structures respond to dynamic loads such as slamming. Fundamentally, FEM represents a continuous structure as an interconnected assembly of discrete elements, each governed by the laws of mechanics. By linking these elements through nodal points and assembling their stiffness relationships, a global system of equations is formed that describes the overall structural behavior in terms of displacements, strains, and stresses [32].

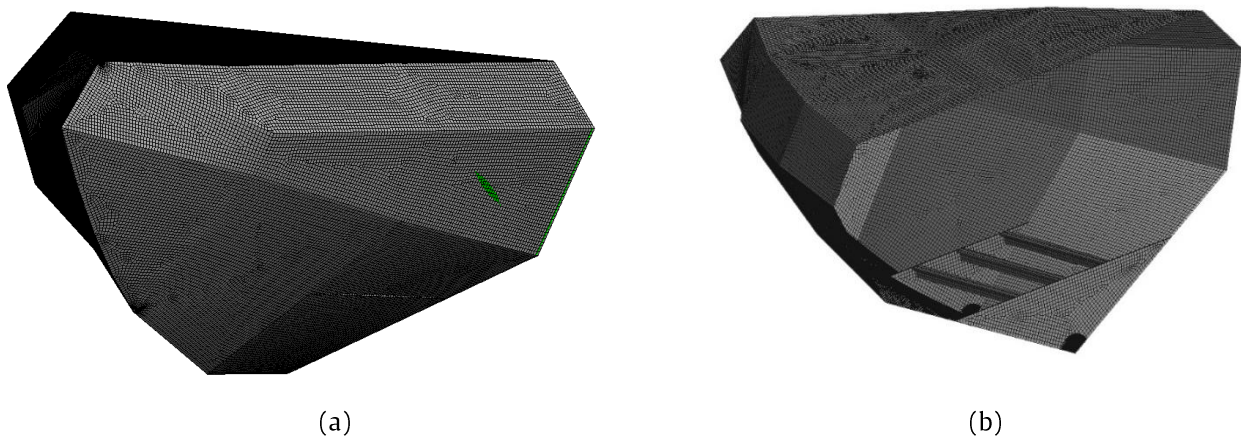


Figure 5. Geometry model of the ship's bow with mesh configuration; (a) Bow viewpoint, (b) Mesh distribution inside the structure

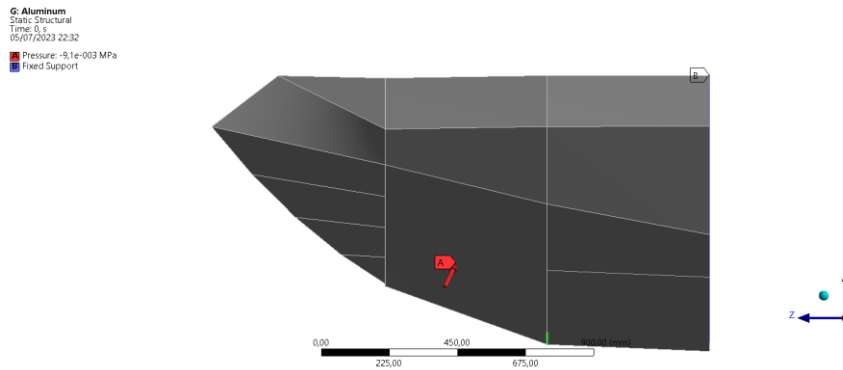


Figure 6. Application of Boundary Constraints in FEM Simulations

In slamming analysis, the hull is discretized into a finite element mesh, allowing the governing elasticity equations to be solved over a complex geometry. External forces caused by wave impact are introduced as surface pressures on boundary regions of the mesh, and equilibrium is enforced to compute nodal displacements. From these, stress and deformation fields can be derived to reveal how sudden, high-magnitude hydrodynamic pressures propagate through the hull [33,34]. This capability makes FEM particularly well suited to marine applications where lightweight materials such as aluminium or sandwich composites must withstand repeated impulsive loading [35,36].

The accuracy of FEM solutions depends on mesh density and element quality, making mesh refinement and convergence studies essential. Finer elements in regions of anticipated stress concentration such as stiffener intersections or cutouts ensure that the numerical model closely reproduces the true structural response [37]. The mesh arrangement for this study is presented in Figure 5, and the corresponding boundary conditions are illustrated in Figure 6.

### 3. Results and Discussion

#### 3.1. Seakeeping and Slamming Probability

Figure 7 presents the Response Amplitude Operator (RAO) curves for heave and pitch motions of the small craft under head, beam, and following seas at zero and 20 kn forward speed. The RAO expresses the ratio of vessel motion amplitude to incident wave amplitude as a function of encounter frequency, thereby identifying the frequencies at which the hull exhibits pronounced dynamic susceptibility. In head seas, the stationary condition produces a dominant low-frequency peak in both heave and pitch, indicating strong vertical and angular responses when long-period waves excite the natural modes of the hull. Increasing the speed to 20 kn amplifies these motions and shifts the peak toward higher encounter frequency owing to Doppler effects and speed-dependent changes in added mass and radiation damping. This behaviour underscores a heightened risk of bow slamming when advancing into oncoming seas.

Under beam-sea excitation, heave remains the principal response while pitch is minimal at rest, reflecting predominantly vertical lift with limited rotational motion. Forward motion sharpens and elevates the heave peak near 4–5  $\text{rad s}^{-1}$ , demonstrating that forward speed enhances vertical resonance when waves impinge laterally, which may intensify bottom-panel loads despite modest pitch. For following seas, both RAOs are negligible when the vessel is stationary. At 20 kn, however, the encounter frequency shifts toward negative values as the craft overtakes the waves, and both heave and pitch RAOs rise near zero frequency, signifying low-frequency but larger-amplitude motions that can promote stern or quartering slamming.

Figure 8 collectively illustrate how wave height, heading, and vessel speed influence heave and pitch responses and the resulting probability of slamming. In the head-sea condition at zero speed, both heave and pitch amplitudes rise steadily with increasing wave height, but pitch grows more sharply. Direct wave impact on the bow induces strong vertical lift and rotational moments, so pitch-related slamming probability surpasses 80% at 0.5 m while heave-related slamming remains below about 40%.

In the beam-sea case at rest, heave increases more than pitch, but overall motions are moderate. Side-wave uplift excites vertical motion while producing only minor bow-up or bow-down rotation, which limits pitch amplitude and keeps pitch slamming probability below roughly 20% even at the highest wave height. For the following-sea condition with no forward motion, ship motions remain small at low wave heights but rise noticeably at 0.5 m. Overtaking waves gently lift the stern, causing the bow to dip into successive crests and producing a pitch-driven slamming probability of about 80%, again higher than that from heave.

When the craft advances to 20 knots in head seas, both heave and pitch responses increase markedly compared with the stationary case. The higher encounter frequency and relative water impact amplify vertical acceleration and rotation, pushing pitch slamming probability beyond 90% at 0.5 m and substantially increasing heave-related risk as well. Under beam seas at 20 knots, heave magnitude nearly doubles relative to the zero-speed case, and heave slamming probability approaches 50%. Forward speed sharpens resonance near 4–5  $\text{rad/s}$ , intensifying vertical motion even with waves striking the hull laterally, while pitch remains limited and its slamming probability stays comparatively low.

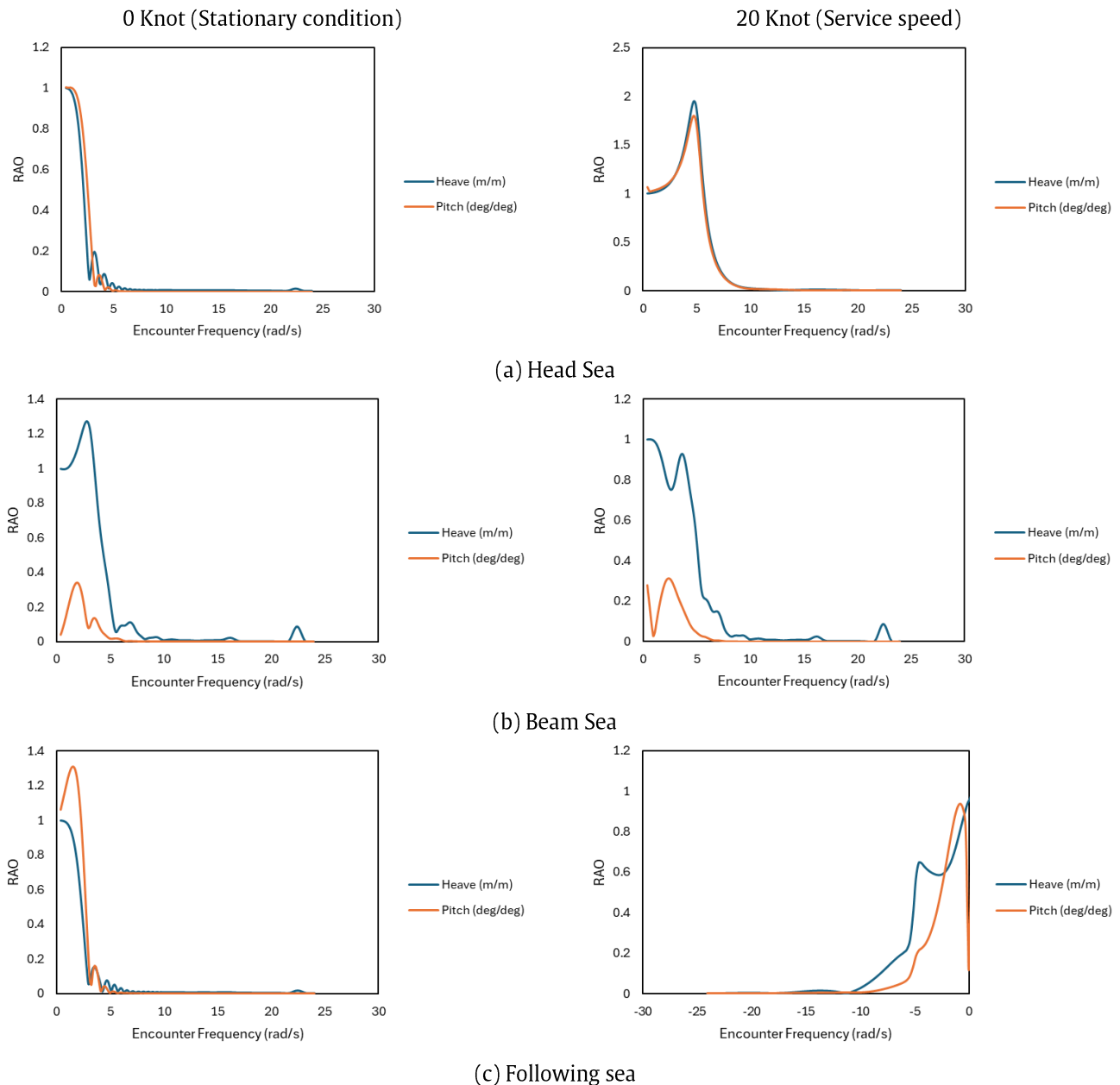


Figure 7. RAO for each vertical motion on wave heading and operational variations

Finally, in following seas at 20 knots, both heave and pitch amplitudes rise relative to the stationary condition, and pitch slamming probability climbs to roughly 60%. As the vessel overtakes wave systems, low encounter frequencies encourage the stern to lift into passing crests, producing stronger bow-down pitch and more pronounced slamming loads at the bow. Overall, pitch consistently emerges as the primary driver of slamming across all headings, while forward speed amplifies both motion responses and slamming probability. These findings highlight the bow bottom as the critical structural area and underscore the operational need to reduce speed when wave heights approach 0.5 m to mitigate slamming-induced loads.

Hydrodynamic loads were assessed through a diffraction-based analysis using the Boundary Element Method (BEM), which models the interaction between incident regular waves and the hull under the assumptions of potential flow [38]. Simulation results, visualized in Figure 9, shows that slamming pressures are consistently concentrated at the bow, the first point of contact with incoming waves, making it the most critical structural zone. Across the tested sea states, the maximum calculated slamming loads reached approximately  $2.28 \times 10^{-3}$  MPa at a 0.125 m wave height,  $4.55 \times 10^{-3}$  MPa at 0.250 m, and  $9.10 \times 10^{-3}$  MPa at 0.500 m, with all peaks occurring along the forward bottom plating where slamming initiates [32].

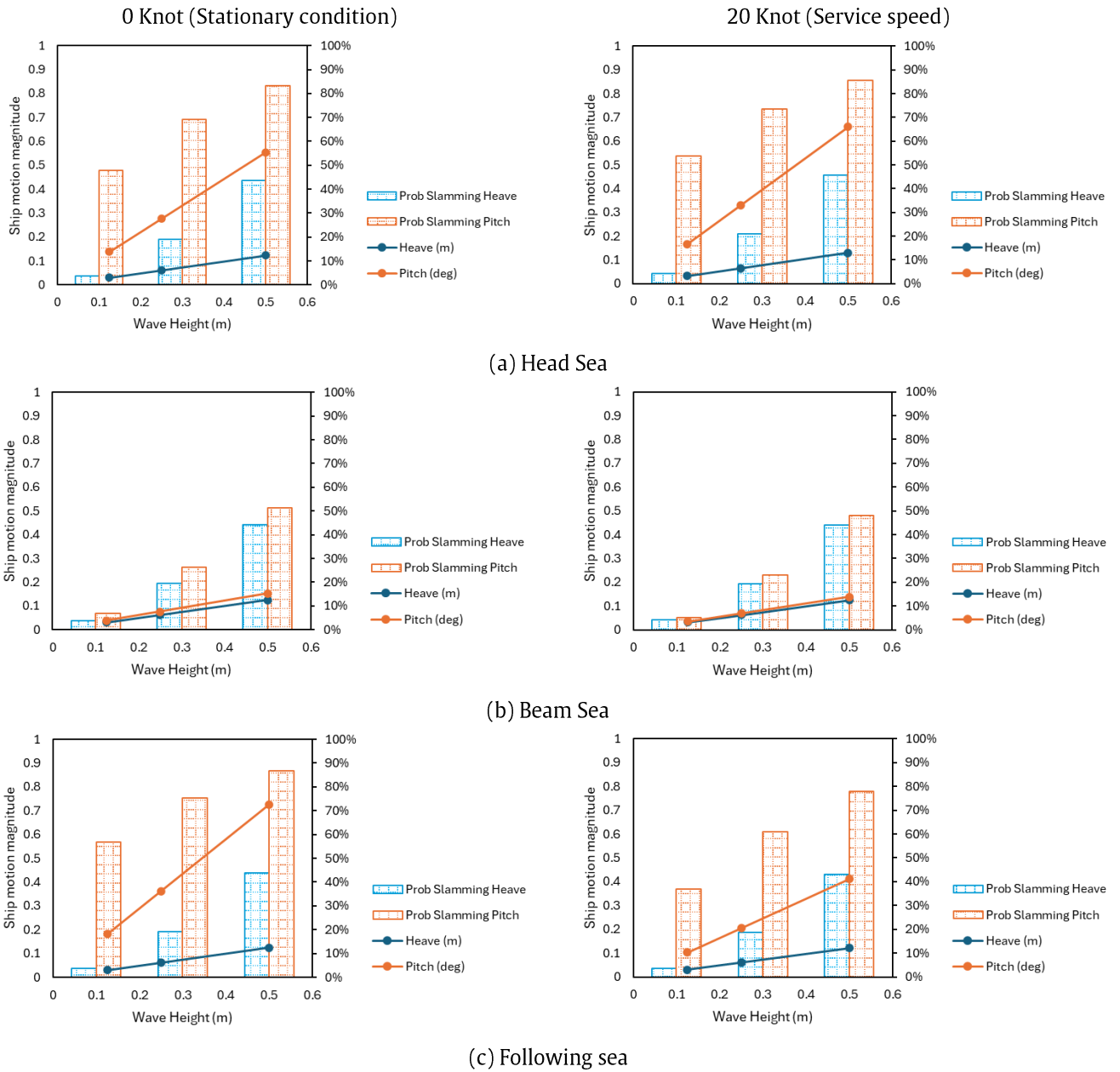
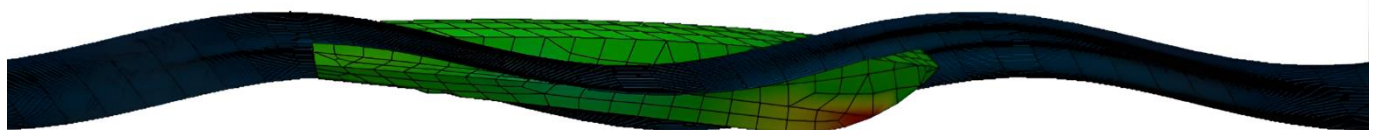
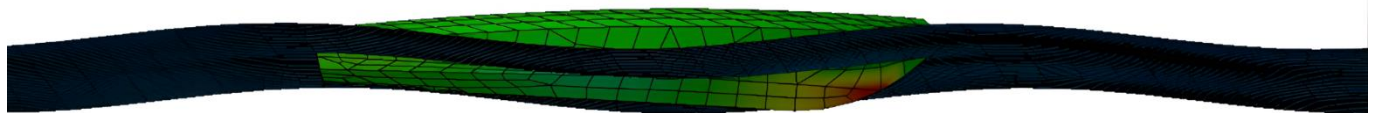
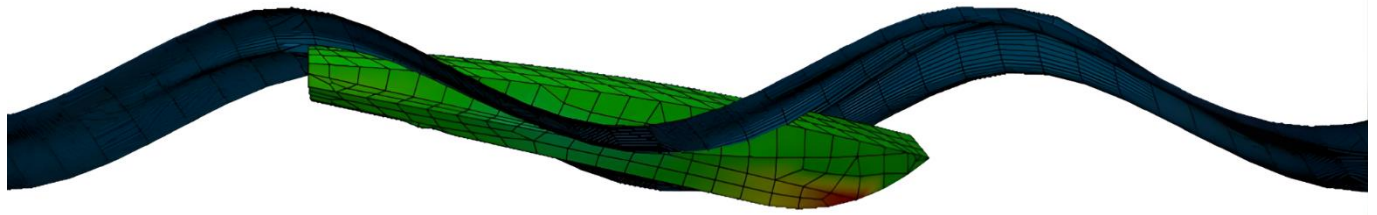


Figure 8. RMS of each vertical motion and each respective slamming probability level





(c) 0.500 m head wave

Figure 9. Visualization of slamming occurrence on the small craft under different wave conditions

### 3.2. Slamming Effect on Hull

The finite element simulations, shown in Figures 10–12 for the range of simulated wave heights, detail how the hull reacts structurally when subjected to slamming impacts. With increasing wave severity, both the stress and the displacement of key hull sections grow noticeably. Contours of equivalent stress reveal maximum values approaching 19 MPa, concentrated along the forward bottom plating where transverse frame support is minimal. These high readings demonstrate that areas without reinforcement are far more susceptible to overload, while zones adjacent to stiffeners exhibit significantly lower stresses, confirming the stiffeners’ role in spreading and dissipating impact forces.

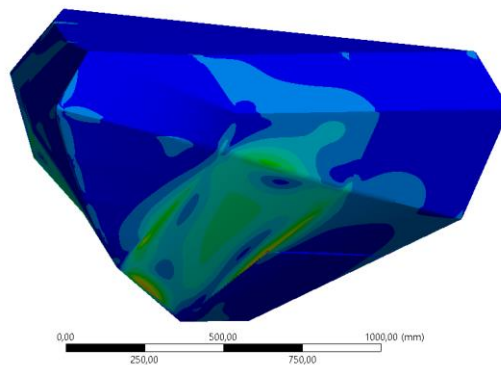
Displacement plots reinforce this pattern: peak out-of-plane movements reach roughly 0.76 mm, forming circular deformation bands across the unsupported plating. Although such deflection remains within allowable limits for aluminium construction, repeated cycles of this magnitude could hasten fatigue damage and shorten service life. The analysis therefore shows that flat plating without adequate framing is much more likely to experience noticeable bending and deflection under impulsive hydrodynamic pressures.

Table 3 summarizes the structural responses, demonstrating a clear, nearly proportional increase in both stress and deformation as slamming intensity rises. Throughout all scenarios, the highest loads and deflections consistently occur in regions lacking transverse reinforcement, whereas stiffened segments display a markedly stronger resistance to impact. Overall, these results highlight that structural configuration particularly the spacing and placement of stiffeners and transverse members has as much influence on vulnerability as the magnitude of the slamming forces themselves. Thoughtful reinforcement design is therefore critical to reduce the risk of local overstressing and to ensure long-term durability of small, high-speed craft operating in energetic seas.

Table 3. Hull Response Across Wave Variations

Wave Height (m)	Stress (MPa)	Deform (mm)
0.125	4.7744	0.19
0.250	9.5278	0.38
0.500	19.056	0.76

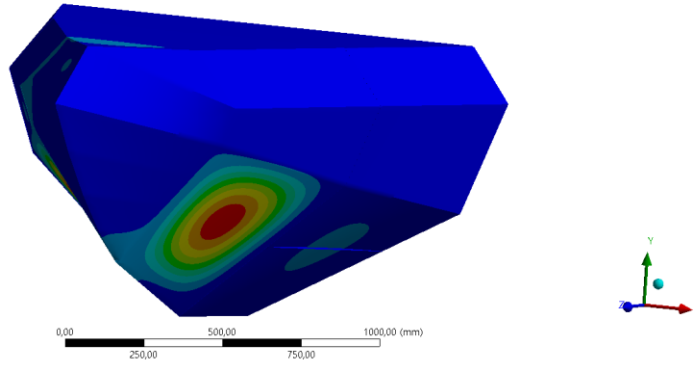
G: Aluminum  
 Equivalent Stress  
 Type: Equivalent (von-Mises) Stress - Top/Bottom  
 Unit: MPa  
 Time: 1 s  
 05/07/2023 22:26  
 4.7744 Max  
 4.2303  
 3.9063  
 3.4723  
 3.0382  
 2.6042  
 2.1702  
 1.7361  
 1.3021  
 0.86807  
 0.43403  
 0 Min



(a) Stress distribution of the structure

G: Aluminum  
Total Deformation  
Type: Total Deformation  
Unit: mm  
Time: 1 s  
05/07/2023 22:26

0.19044 Max
0.16928
0.14812
0.12696
0.1058
0.084638
0.063478
0.042319
0.021159
0 Min

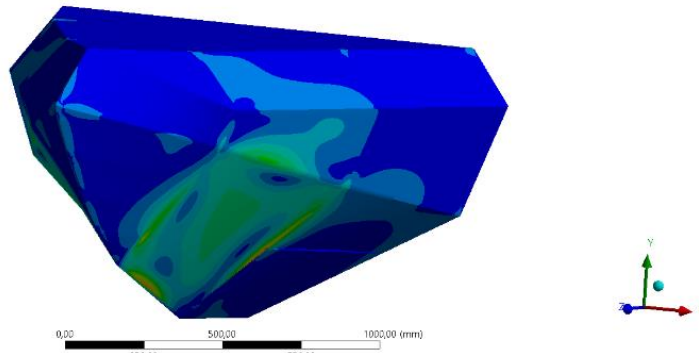


(b) Deformation of the structure

Figure 10. Aluminum Speedboat Structure to 0.125 m Slamming Loads

G: Aluminum  
Equivalent Stress  
Type: Equivalent (von-Mises) Stress - Top/Bottom  
Unit: MPa  
Time: 1 s  
05/07/2023 22:24

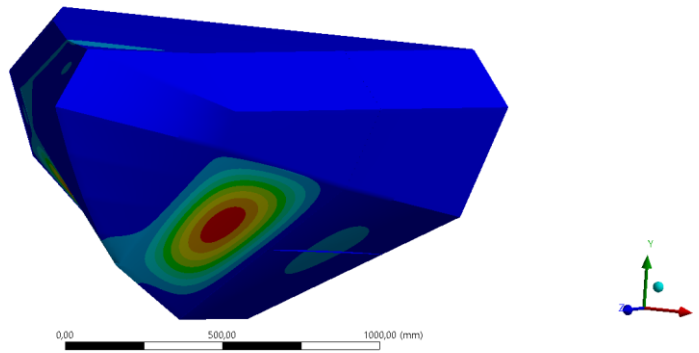
9.5278 Max
8.6616
7.7955
6.9293
6.0631
5.197
4.3308
3.4647
2.5985
1.7323
0.86616
0 Min



(a) Stress distribution of the structure

G: Aluminum  
Total Deformation  
Type: Total Deformation  
Unit: mm  
Time: 1 s  
05/07/2023 22:25

0.38004 Max
0.33781
0.29558
0.25336
0.21113
0.1689
0.12668
0.084452
0.042226
0 Min

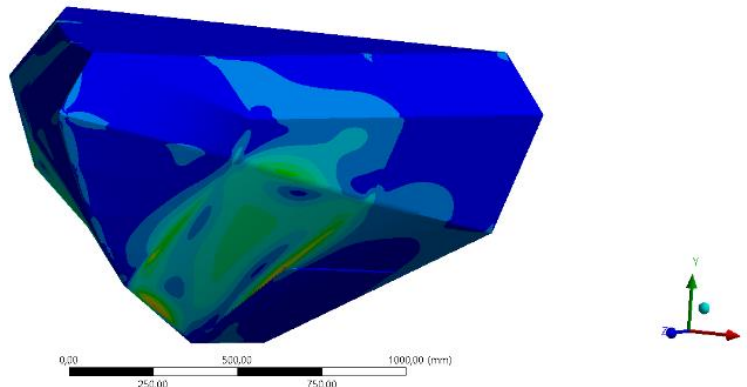


(b) Deformation of the structure

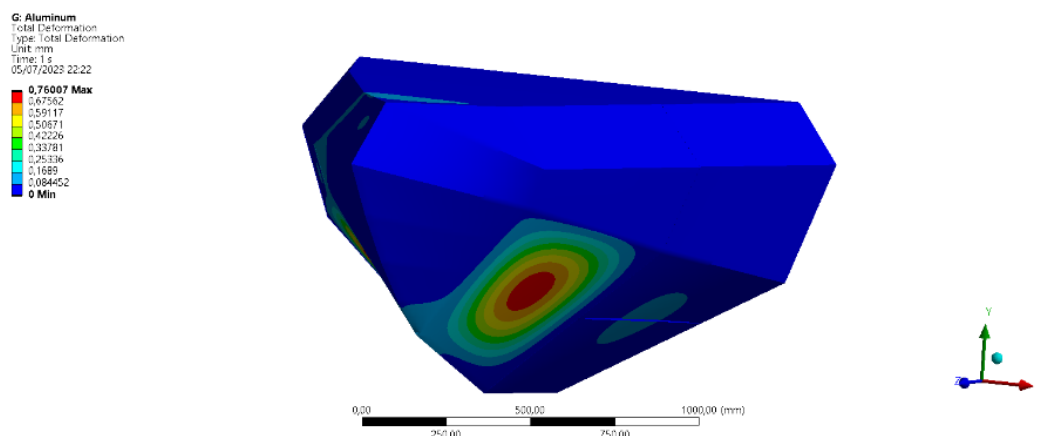
Figure 11. Aluminum Speedboat Structure to 0.25 m Slamming Loads

G: Aluminum  
Equivalent Stress  
Type: Equivalent (von-Mises) Stress - Top/Bottom  
Unit: MPa  
Time: 1 s  
05/07/2023 22:29

19.056 Max
17.223
15.391
13.559
12.726
10.894
9.0616
7.2293
5.397
3.5647
1.7323
0 Min



(a) Stress distribution of the structure



(b) Deformation of the structure

Figure 12. Aluminum Speedboat Structure to 0.5 m Slamming Loads

#### 4. Conclusion

This study provides a comprehensive assessment of the slamming probability and structural response of an aluminum speedboat, combining seakeeping motion analysis with finite element structural evaluation. By applying the Boundary Element Method (BEM), the vessel's heave and pitch motions under regular wave conditions were accurately predicted and used to estimate the likelihood of bottom slamming. The results clearly show that pitch motion is the dominant driver of slamming, with the probability of occurrence rising from 54 % at 0.125 m significant wave height to 86 % at 0.50 m, while the heave-related probability increased from 4 % to 46 % over the same range. These findings indicate that even moderate increases in wave height can dramatically elevate the risk of severe hull impacts.

The hydrodynamic pressures derived from the seakeeping analysis were applied to a detailed Finite Element Method (FEM) model of the hull to evaluate structural stresses and deformations. As slamming loads intensified, the hull experienced a proportional increase in structural response: maximum equivalent stress climbed from about 4.8 MPa at 0.125 m wave height to nearly 19 MPa at 0.50 m, while peak deformation grew from 0.19 mm to 0.76 mm. Stress contour plots consistently identified the forward bottom plating near the bow as the critical region, particularly in areas not supported by transverse frames. In contrast, panels adjacent to stiffeners and transverse members maintained significantly lower stress levels, confirming the importance of reinforcement layout in distributing impact loads and reducing localized overstress.

These results emphasize that structural design and sea-state severity jointly govern the vulnerability of small, high-speed craft to slamming. The combination of high pitch motion and insufficient reinforcement can lead to rapid fatigue accumulation, local buckling, or even fracture if repeated impacts occur. From a design perspective, strengthening unsupported plating, optimizing stiffener spacing, and considering alternative lightweight materials—such as sandwich composites—can markedly improve structural resilience. Operationally, avoiding prolonged exposure to sea states that generate encounter frequencies near the vessel's natural pitch resonance, or adjusting speed to reduce relative motion, will further lower slamming risk.

#### Acknowledgment

The authors gratefully acknowledge the support provided by Institut Teknologi Kalimantan (ITK) and Universitas Diponegoro (UNDIP) for providing the facilities and support that made this research possible.

#### References

- [1] T. Rahmaji, A. R. Prabowo, T. Tuswan, T. Muttaqie, N. Muhyat, and S.-J. Baek, "Design of Fast Patrol Boat for Improving Resistance, Stability, and Seakeeping Performance," *Designs (Basel)*, vol. 6, no. 6, p. 105, Nov. 2022, doi: <https://doi.org/10.3390/designs6060105>.
- [2] S. Pegorari, "The Effect of Slamming on Composite Boats," Metstrade.
- [3] R. S. Thodal, *On Full Scale Slamming Testing of High-Speed Boats*. United States: Lehigh University, 2016.
- [4] D. D. Truong, B.-S. Jang, H.-B. Ju, and S. W. Han, "Prediction of slamming pressure considering fluid-structure interaction. Part II: Derivation of empirical formulations," *Marine Structures*, vol. 75, p. 102700, Jan. 2021, doi: <https://doi.org/10.1016/j.marstruc.2019.102700>.
- [5] L. S. Gao and P. Zhou, "Three-dimensional simulation of ship bow slamming," *E3S Web of Conferences*, vol. 261, p. 03031, May 2021, doi: <https://doi.org/10.1051/e3sconf/202126103031>.
- [6] S. S. Mousavi and A. Askarian Khoob, "Effect of Ultra-Lightweight High-Ductility Cementitious Composite in Steel-Concrete-Steel (SCS) Plate to Mitigate Ship Slamming Loads," *Journal of Composites Science*, vol. 7, no. 8, p. 331, Aug. 2023, doi: <https://doi.org/10.3390/jcs7080331>.
- [7] H. Li, J. Zou, B. Deng, R. Liu, and S. Sun, "Experimental study of stern slamming and global response of a large cruise ship in regular waves," *Marine Structures*, vol. 86, p. 103294, Nov. 2022, doi: <https://doi.org/10.1016/j.marstruc.2022.103294>.

- [8] D. D. Truong, B.-S. Jang, H.-B. Ju, and S. W. Han, "Prediction of slamming pressure considering fluid-structure interaction. Part I: numerical simulations," *Ships and Offshore Structures*, vol. 17, no. 1, pp. 7–28, Jan. 2022, doi: <https://doi.org/10.1080/17445302.2020.1816732>.
- [9] A. I. Wulandari, A. Sulisetyono, and I. K. A. P. Utama, "The influence of hull and tunnel geometry on resistance and seakeeping behavior of flat side-inside catamaran," *Ships and Offshore Structures*, pp. 1–35, Jul. 2025, doi: <https://doi.org/10.1080/17445302.2025.2529968>.
- [10] A. I. Wulandari, A. Alamsyah, S. Suardi, W. Setawan, M. U. Pawara, A. M. N. Arifudin, H. Syahab, "Material Reliability Study of High-Speed Small Craft Under Wave Load," *Journal of Marine-Earth Science and Technology*, vol. 5, no. 3, pp. 74–86, 2025, doi: <https://doi.org/10.12962/j27745449.v5i3.3921>
- [11] A. I. Wulandari, H. Syahab, A. Baidowi, and B. A. Adietya, "Structural Response Analysis During Slamming Events on Speedboats Using Aluminum Material," *International Journal of Marine Engineering Innovation and Research*, vol. 10, no. 3, pp. 971–979, 2025, doi: <https://doi.org/10.12962/j25481479.v10i3>
- [12] M. I. Jifaturrohman, I. K. A. P. Utama, T. Putranto, D. Setyawan, and L. Huang, "A study into the correlation between single array-hull configurations and wave spectrum for floating solar photovoltaic systems," *Ocean Engineering*, vol. 312, p. 119312, Nov. 2024, doi: <https://doi.org/10.1016/j.oceaneng.2024.119312>.
- [13] M. A. Wahid, A. N. Siddiquee, and Z. A. Khan, "Aluminum alloys in marine construction: characteristics, application, and problems from a fabrication viewpoint," *Marine Systems & Ocean Technology*, vol. 15, no. 1, pp. 70–80, Mar. 2020, doi: <https://doi.org/10.1007/s40868-019-00069-w>.
- [14] AmesWeb, "Aluminium ALloys - Yield Strength and Tensile Strength," AmesWeb.
- [15] ASM, "Aluminum 6061-T6; 6061-T651," [asm.matweb.com](http://asm.matweb.com).
- [16] Gabrian International, "6061 Aluminum: Get to Know its Properties and Uses," Gabrian International.
- [17] Ferguson Perforating, "6061 Aluminium Alloy," [fergusonperf.com](http://fergusonperf.com).
- [18] AZO Materials, "Aluminium: Specifications, Properties, Classifications and Classes," [azom.com](http://azom.com).
- [19] O. F. Hosseinabadi, M. R. Khedmati, and M. Norouzipoor, "Statistical analysis of initial deflection of aluminium plating between stiffeners," *Thin-Walled Structures*, vol. 161, p. 107528, Apr. 2021, doi: <https://doi.org/10.1016/j.tws.2021.107528>.
- [20] Riswanda, Akhyar, Sugianto, H. Kadir, and S. Rizal, "Numerical Simulation of the Effect of Shoulder Rotation on the Tensile Strength of FSW Dissimilar Joints of Aluminum Alloy," *Defect and Diffusion Forum*, vol. 402, pp. 90–99, Jul. 2020, doi: <https://doi.org/10.4028/www.scientific.net/DDF.402.90>.
- [21] O. F. Hughes and J. K. Paik, *Ship Structural Analysis and Design*. New Jersey: Society of Naval Architects and Marine Engineers, 2010.
- [22] BMKG, "BMKG Ocean Forecast System," 2023, *Badan Meteorologi Klimatologi dan Geofisika*.
- [23] R. Datta and C. Guedes Soares, "Analysis of the hydroelastic effect on a container vessel using coupled BEM–FEM method in the time domain," *Ships and Offshore Structures*, vol. 15, no. 4, pp. 393–402, Apr. 2020, doi: <https://doi.org/10.1080/17445302.2019.1625848>.
- [24] T. Bunnik, D. Van, G. kapsenberg, Y. Shin, R. Huijsmans, G. B. Deng, G. Delhommeau, M. Kashiwagi, B. Beck, "A comparative study on state-of-the-art prediction tools for seakeeping," *28th Symposium on Naval Hydrodynamics, Pasadena, California, USA*, 2010.
- [25] U.-J. Lee, W.-M. Jeong, and H.-Y. Cho, "Estimation and Analysis of JONSWAP Spectrum Parameter Using Observed Data around Korean Coast," *Journal of Marine Science and Engineering*, vol. 10, no. 5, p. 578, Apr. 2022, doi: <https://doi.org/10.3390/jmse10050578>.
- [26] T. G. Tran, V. T. Doan, and H. Tran, "A new approach to improving the accuracy of seakeeping predictions using strip theory for high-speed vessels," *Ocean Engineering*, vol. 327, p. 120995, May 2025, doi: <https://doi.org/10.1016/j.oceaneng.2025.120995>.
- [27] S. Bielicki, "Prediction of Ship Motions in Irregular Waves Based on Response Amplitude Operators Evaluated Experimentally in Noise Waves," *Polish Maritime Research*, vol. 28, no. 1, pp. 16–27, Mar. 2021, doi: <https://doi.org/10.2478/pomr-2021-0002>.
- [28] H. K. Versteeg and W. Malalasekera, *An Introduction to Computational Fluid Dynamics the Finite Volume Method*. London: Pearson Education Limited, 2007.
- [29] A. Ion and I. Ticu, "The finite element method for calculating the marine structural design," in *IOP Conference Series: Materials Science and Engineering*, Institute of Physics Publishing, Nov. 2015. doi: <https://doi.org/10.1088/1757-899X/95/1/012073>.
- [30] T. Tuswan, K. Abdullah, A. Zubaydi, and A. Budipriyanto, "Finite-element Analysis for Structural Strength Assessment of Marine Sandwich Material on Ship Side-shell Structure," *Materials Today Proceeding*, vol. 13, pp. 109–114, Jan. 2019, doi: <https://doi.org/10.1016/J.MATPR.2019.03.197>.
- [31] B. W. Lenggana *et al.*, "Effects of mechanical vibration on designed steel-based plate geometries: behavioral estimation subjected to applied material classes using finite-element method," *Curved and Layered Structures*, vol. 8, no. 1, pp. 225–240, Jan. 2021, doi: <https://doi.org/10.1515/cls-2021-0021>.
- [32] D. L. Logan, *A First Course in the Finite Element Method*, 6th ed. Boston: Cengage Learning, 2015.
- [33] H. Syahab, A. Zubaydi, H. Siswanti, and R. C. Ariesta, "Failure Behavior Analysis of Crack Propagation in Ship Sandwich Structures," *Scientific Journal of Maritime Research – Pomorstvo (Accepted to be Published)*, 2025.
- [34] H. Syahab *et al.*, "Structural design evaluation for Underwater Remotely Operated Vehicle (ROV), case study: Madura Straits," 2022.

- [35] R. C. Ariesta, A. Zubaydi, A. Ismail, Tuswan, and M. Z. Al-Syachri, "Identification of damage in a ship hull sandwich plate by natural frequency," *IOP Conference Series: Materials Science and Engineering*, vol. 1034, no. 1, p. 012012, Feb. 2021, doi: <https://doi.org/10.1088/1757-899X/1034/1/012012>.
- [36] M. N. Misbah, D. Setyawan, T. Yulianto, R. C. Ariesta, and W. H. A. Putra, "Stress Concentration Analysis on Ship Plate with Hole using Numerical Approach," in *Proceedings of the 4th International Conference on Marine Technology*, SCITEPRESS - Science and Technology Publications, 2019, pp. 117–121. doi: <https://doi.org/10.5220/0010855200003261>.
- [37] M. S. Akbar, A. R. Prabowo, D. D. D. Prija Tjahjana, F. B. Laksono, and S. J. Baek, "Assessment of Designed Midship Section Structures subjected to the Hydrostatic and Hydrodynamic Loads: A Convergence Study," *Procedia Structural Integrity*, vol. 33, pp. 67–74, 2021, doi: <https://doi.org/10.1016/j.prostr.2021.10.010>.
- [38] M. A. Hafiz and A. Sulisetyono, "Structural Reliability Analysis for the Construction Design of the High-Speed Ship with CFRP Material," *IOP Conference Series: Earth and Environmental Science*, vol. 1081, no. 1, p. 012041, Sep. 2022, doi: <https://doi.org/10.1088/1755-1315/1081/1/012041>.